Inorg. Chem. **2007**, *46*, 2691–2699

Sulfur Ligand Substitution at the Nickel(II) Sites of Cubane-Type and Cubanoid $NiFe_3S_4$ Clusters Relevant to the C-Clusters of Carbon Monoxide Dehydrogenase

Jibin Sun, Christian Tessier, and R. H. Holm*

Department of Chemistry and Chemical Biology, Harvard University, Cambridge, Massachusetts 02138

Received December 11, 2006

Substitution reactions at the nickel site of the cubane-type cluster $[(Ph_3P)NiFe_3S_4(LS_3)]^{2-}$ (**2**) have been investigated in the course of a synthetic approach to the C-clusters of CODH. Reaction of **2** with RS^- or toluene-3,4-dithiolate affords $[(RS)NiFe_3S_4(LS_3)]^{3-}$ (R = Et (**5**), H (**6**)) or $[(tdt)NiFe_3S_4(LS_3)]^{3-}$ (**7**), demonstrating that anionic sulfur ligands can be bound at the Ni^{II} site. Clusters **5** and **6** contain tetrahedral $Ni(\mu_3\text{-}S)_3(SR)$ sites. Cluster **7** is of particular interest because it includes a cubanoid $NiFe_3(\mu_2\text{-}S)(\mu_3\text{-}S)_3$ core and an approximately planar $Ni(tdt)(\mu_3\text{-}S)_2$ unit. The cubanoid structure is found in all C-clusters, and an NiS_4-type unit has been reported in *C. hydrogenoformans* CODH. Clusters **5**/**6** are formulated to contain the core $[NiFe_3S_4]^{1+} \equiv Ni^{2+}$ ($S = 1$) + $[Fe_3S_4]^{1-}$ ($S = 5/2$) and **7** the core $[NiFe_3S_4]^{2+} \equiv Ni^{2+}$ ($S = 0$) + $[Fe_3S_4]^0$ ($S = 2$) on the basis of structure, ^{57}Fe isomer shifts, and ^1H NMR isotropic shifts. Also reported are $[(EtS)CuFe_3S_4(LS_3)]^{3-}$ (**9**) and $[Fe_4S_4(LS_3)(tdt)]^{3-}$ (**11**). The structures of **5**–**7**, **9**, and **11** are presented. Cluster **11**, with a five-coordinate $Fe(tdt)(\mu_3\text{-}S)_3$ site, provides a clear structural contrast with **7**, which is currently the closest approach to a C-cluster but lacks the exo iron atom found in the $NiFe_4S_{4,5}$ cores of the native clusters. (CODH = carbon monoxide dehydrogenase, LS_3 = 1,3,5-tris((4,6-dimethyl-3-mercaptophenyl)thio)-2,4,6-tris(*p*-tolylthio)benzene(3–), tdt = toluene-3,4-dithiolate)

Introduction

The C-cluster of carbon monoxide dehydrogenase[1−3] is the site of the reaction $CO + H_2O = CO_2 + 2H^+ + 2e^-$ whereby CO is oxidized and CO_2 is reduced in methanogenic archaea and acetogenic and anaerobic bacteria. CODHs[4] are implicated in the Wood−Lungdahl pathway of acetate synthesis. In bifunctional enzymes, carbon monoxide produced at the C-cluster appears at the A-cluster by means of a tunneling pathway[5,6] where it is utilized in acetylcoenzyme A synthase activity. Considerable interest attends the structural and electronic properties of the catalytic sites of this enzyme. The crystallographically determined structures of the C-clusters from three sources contain a cubanoid $NiFe_3S_4$ entity to which is bridged an exo iron atom.[7−10] These structures differ in the details of nickel and exo iron ligation, and several are complicated by partial atom occupancies and disordered positions. Summaries of these structures are available elsewhere.[11−13]

In our continuing efforts on the synthesis of weak-field cluster analogues of biological sites,[14,15] we have taken as one objective the C-cluster of CODH. As a definite target,

* To whom correspondence should be addressed. E-mail: holm@chemistry.harvard.edu.

(1) Ragsdale, S. W.; Kumar, M. *Chem. Rev.* **1996**, *96*, 2515−2539.
(2) Lindahl, P. A. *Biochemistry* **2002**, *41*, 2097−2105.
(3) Ragsdale, S. W. *Crit. Rev. Biochem. Mol. Biol.* **2004**, *39*, 165−195.
(4) Abbreviations are given in the chart.
(5) Tan, X.; Loke, H.-K.; Fitch, S.; Lindahl, P. A. *J. Am. Chem. Soc.* **2005**, *127*, 5833−5839.
(6) Volbeda, A.; Fontecilla-Camps, J. C. *J. Biol. Inorg. Chem.* **2004**, *9*, 525−532.
(7) Dobbek, H.; Svetlitchnyi, V.; Gremer, L.; Huber, R.; Meyer, O. *Science* **2001**, *293*, 1281−1285.
(8) Dobbek, H.; Svetlitchnyi, V.; Liss, J.; Meyer, O. *J. Am. Chem. Soc.* **2004**, *126*, 5382−5387.
(9) Drennan, C. L.; Heo, J.; Sintchak, M. D.; Schreiter, E.; Ludden, P. W. *Proc. Natl. Acad. Sci. U.S.A.* **2001**, *98*, 11973−11978.
(10) Doukov, T. I.; Iverson, T. M.; Seravalli, J.; Ragsdale, S. W.; Drennan, C. L. *Science* **2002**, *298*, 567−572.
(11) Drennan, C. L.; Peters, J. W. *Curr. Opin. Struct. Biol.* **2003**, *13*, 220−226.
(12) Drennan, C. L.; Doukov, T. I.; Ragsdale, S. W. *J. Biol. Inorg. Chem.* **2004**, *9*, 511−515.
(13) Volbeda, A.; Fontecilla-Camps, J. C. *J. Chem. Soc. Dalton Trans.* **2005**, 3443−3450.
(14) Lee, S. C.; Holm, R. H. *Proc. Natl. Acad. Sci. U.S.A.* **2003**, *100*, 3595−3600.
(15) Lee, S. C.; Holm, R. H. *Chem. Rev.* **2004**, *104*, 1135−1157.

10.1021/ic062362z CCC: $37.00
Published on Web 03/09/2007

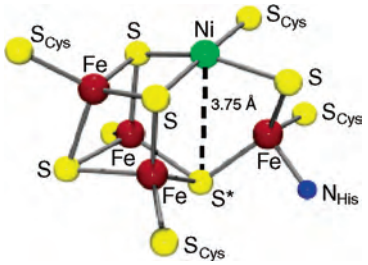

Figure 1. Structure of the C-cluster of dithionite-reduced *C. hydrogenoformans* CODH II at 1.1 Å, resolution.

we have selected the cluster from *Carboxydothermus hydrogenoformans*. The structure of the cluster in dithionite-reduced *Ch* CODH II determined at 1.1 Å resolution is shown in Figure 1.[8] The structure consists of a cuboidal Fe_3S_4 fragment with tetrahedral iron sites to which is bound a nickel atom in an approximately planar configuration separated from an axial sulfur atom S* at 3.75 Å. A tetrahedral iron atom is bridged to the $NiFe_3S_4$ entity by two sulfide bridges, resulting in a cluster with the $NiFe_4S_5 = NiFe_4(\mu_2\text{-}S)(\mu_3\text{-}S)_4$ core. No synthetic or other native M−Fe−S cluster of this construction is known. Synthesis of the desired cluster involves at least two steps: (i) stabilization of planar four-coordinate nickel site in an $NiFe_3S_4$ cluster unit and (ii) binding of an exo iron atom to this unit. In previous work, we have accomplished step (i) by means of reaction 1, in which the strong in-plane chelate ligand dmpe promotes a planar Ni^{II} stereochemistry.[16,17] The reaction proceeds with a $S = 3/2 \rightarrow S = 5/2$ ground-state spin change upon creation of the diamagnetic $Ni^{II}P_2S_2$ site within the $[NiFe_3S_4]^{1+}$ core from a tetrahedral $Ni^{II}PS_3$ site. Analogous clusters containing Pd^{II} and Pt^{II} have also been synthesized and structurally characterized.[17]

$$[(Ph_3P)NiFe_3S_4(LS_3)]^{2-} + \text{dmpe} \rightarrow [(\text{dmpe})NiFe_3S_4(LS_3)]^{2-} + Ph_3P \quad (1)$$

Given the $Ni(\mu_2\text{-}S)(\mu_3\text{-}S)_2(S_{Cys})$ unit reported in *Ch* CODH II, a desirable next step is the achievement of a planar Ni^{II} site stabilized by all-sulfur coordination that includes ligand atoms possibly capable of bridging to an exo iron atom. Consequently, we have sought additional substitution reactions at the nickel site that introduce ligands of more physiological relevance with the potential of bridge formation. The initial results of this research are described here.

Experimental Section

Preparation of Compounds. All reactions and manipulations were performed under a pure dinitrogen atmosphere using either Schlenk techniques or an inert-atmosphere box. Solvents were passed through an Innovative Technology solvent purification system prior to use. Volume reduction and drying steps were carried out in vacuo. Because of the small scale of the preparations, products were characterized by physical methods. The five cluster compounds in Table 1 were identified by X-ray structure determinations. In addition, all clusters display well-resolved isotropically shifted ^{1}H NMR spectra which, in conjunction with spectra of known compounds of the types $[L'MFe_3S_4(LS_3)]^z$ (M = Ni,[16−18] Cu[18]) and $[Fe_4S_4(LS_3)L']^z$,[19] serve to identify them and are indicative of substantial purity of isolated compounds. Several compounds exhibited species in their electrospray mass spectra consistent with intact clusters (M = cluster).

$(Et_4N)(SEt)$. To a solution of 1.00 g (11.9 mmol) of NaSEt in 100 mL of acetonitrile was added 1.97 g (11.9 mmol) of Et_4NCl. The solution was stirred for 2 days and filtered through Celite. Removal of solvent gave the product as 1.82 g (80%) of a white microcrystalline solid, which from the ^{1}H NMR spectrum was sufficiently pure to be used without further purification. ^{1}H NMR (CD_3CN): δ 1.13 (t, 3), 1.21 (t, 12), 2.37 (q, 2), 3.24 (q, 8).

$(Et_4N)_2(tdt)$. To a solution of 100 mg (0.50 mmol) of $Na_2(tdt)$ in 50 mL of methanol was added 166 mg (1.00 mmol) of Et_4NCl. The solution was stirred for 20 min, and solvent was removed. The solid residue was extracted with 30 mL of acetonitrile, and the extract was filtered through celite. Solvent was removed from the filtrate to give the product as 174 mg (84%) of a white solid, sufficiently pure by ^{1}H NMR to be used without further purification. ^{1}H NMR (CD_3CN): δ 1.17 (t, 24), 2.07 (s, 3), 3.16 (q, 16), 6.30 (br, 1), 7.13 (d, 2), 7.15 (s, 1).

$(Et_4N)_2[(Ph_3P)NiFe_3S_4(LS_3)]$. To a solution of 250 mg (0.15 mmol) of $(Et_4N)_3[Fe_3S_4(LS_3)]$[20] in 50 mL of acetonitrile was added 46.3 mg (0.17 mmol) of $[Ni(cod)_2]$ followed by 44.1 mg (0.17 mmol) of Ph_3P in 10 mL of acetonitrile. The reaction mixture was stirred for 3 h and filtered. Solvent was removed from the filtrate; the solid residue was washed with ether (3 × 10 mL) and dried. The product was obtained as 220 mg (79%) of black solid, whose ^{1}H NMR spectrum is identical with that reported for this compound prepared by a different method.[18]

$(Et_4N)_3[(EtS)NiFe_3S_4(LS_3)]$. To a solution of 50 mg (27 μmol) of $(Et_4N)_2[(Ph_3P)NiFe_3S_4(LS_3)]$ in 30 mL of acetonitrile was added 25 mg (131 μmol) of $(Et_4N)(SEt)$. The reaction mixture was stirred for 12 h and filtered, and the solvent was removed from the filtrate. The solid residue was washed with cold acetonitrile (−30 °C) and dried, yielding the product as 41 mg (85%) of a black solid. ESMS: *m/z* 1882.8 $\{M + 4Et_4N\}^+$. ^{1}H NMR (Me_2SO-d_6, anion): δ −45.0 (br, SCH_2), 2.23 (4′-Me), 5.12 (SCH_2Me); 6.16, 7.14 (2′-,3′-H); 7.55, 10.60 (4-,6-Me), 14.33 (5-H).

$(Et_4N)_3[(HS)NiFe_3S_4(LS_3)]$. To a solution of 35 mg (19.0 μmol) of $(Et_4N)_2[(Ph_3P)NiFe_3S_4(LS_3)]$ in 20 mL of acetonitrile was added 15 mg (92.0 μmol) of Et_4NSH. The reaction mixture was stirred overnight at room temperature, and the solvent was removed. The solid residue was washed with cold acetonitrile (5 mL, −30 °C), THF (10 mL), and ether (10 mL) and dried to give the product as 25 mg (76%) of a black powder. ^{1}H NMR (Me_2SO-d_6, anion): 2.20 (4′-Me); 6.15, 7.17 (2′-,3′-H), 7.60, 10.74 (4-,6-Me), 14.33 (5-H).

$(Et_4N)_3[(tdt)NiFe_3S_4(LS_3)]$. To a solution of 50 mg (27.0 μmol) of $(Et_4N)_2[(Ph_3P)NiFe_3S_4(LS_3)]$ in 40 mL of acetonitrile was added 60 mg (145 μmol) of $(Et_4N)_2(tdt)$. The reaction mixture was stirred for 90 min. The precipitate was collected by filtration, washed thoroughly with acetonitrile and THF, and dried. The product was obtained as 33 mg (65%) of a black solid. ^{1}H NMR (Me_2SO-d_6,

(16) Panda, R.; Zhang, Y.; McLauchlan, C. C.; Rao, P. V.; Tiago, de Oliveira, F. A.; Münck, E.; Holm, R. H. *J. Am. Chem. Soc.* **2004**, *126*, 6448−6459.
(17) Panda, R.; Berlinguette, C. P.; Zhang, Y.; Holm, R. H. *J. Am. Chem. Soc.* **2005**, *127*, 11092−11101.
(18) Zhou, J.; Raebiger, J. W.; Crawford, C. A.; Holm, R. H. *J. Am. Chem. Soc.* **1997**, *119*, 6242−6250.
(19) Ciurli, S.; Carrié, M.; Weigel, J. A.; Carney, M. J.; Stack, T. D. P.; Papaefthymiou, G. C.; Holm, R. H. *J. Am. Chem. Soc.* **1990**, *112*, 2654−2664.
(20) Zhou, J.; Hu, Z.; Münck, E.; Holm, R. H. *J. Am. Chem. Soc.* **1996**, *118*, 1966−1980.

Table 1. Crystallographic Data for Compounds Containing Clusters **5**, **6**, **7**, **9**, and **11**[a]

	$(Et_4N)_3$[**5**]·2Me_2SO	$(Et_4N)_3$[**6**]·Me_2SO	$(Et_4N)_3$[**7**]·3/4Me_2SO	$(Et_4N)_3$[**9**]·2Me_2SO	$(Et_4N)_3$[**11**]·2Me_2SO
formula[b]	$C_{81}H_{122}Fe_3N_3NiO_2S_{16}$	$C_{77}H_{111}Fe_3N_3NiOS_{15}$	$C_{334}H_{462}Fe_{12}N_{12}Ni_4O_3S_{63}$	$C_{81}H_{122}CuFe_3N_3O_2S_{16}$	$C_{86}H_{123}Fe_4N_3O_2S_{17}$
fw	1909.04	1801.85	7617.98	1913.87	1999.29
cryst syst	monoclinic	orthorhombic	triclinic	monoclinic	monoclinic
space group	$P2_1/c$	$P2_12_12_1$	$P\bar{1}$	$P2_1/n$	$P2_1/n$
Z	4	4	1	4	4
a, Å	19.149(3)	14.650(1)	14.517(1)	19.167(2)	14.127(2)
b, Å	14.280(2)	18.660(2)	19.528(2)	14.204(2)	35.084(6)
c, Å	34.059(4)	34.069(3)	33.269(2)	34.125(4)	19.619(3)
α, deg	90	90	89.047(4)	90	90
β, deg	92.287(3)	90	86.254(4)	92.319(3)	99.803(4)
γ, deg	90	90	87.217(4)	90	90
V, Å^3	9306(2)	9313(1)	9400(1)	9282(2)	9581(3)
GOF (F^2)	0.780	0.780	0.880	0.818	1.012
R1[c] (wR2)[d]	0.0485 (0.918)	0.0545 (0.122)	0.0903 (0.210)	0.0575 (0.109)	0.0708 (0.166)

[a] Data were collected using Mo Kα radiation ($\lambda = 0.71073$ Å) at 193 K. [b] The formula is multiplied so that an integer number of solvent molecules is obtained. [c] $R1 = \sum||F_o| - |F_c||/\sum|F_o|$. [d] $wR2 = \{\sum[w(F_o^2 - F_c^2)^2/\sum[w(F_o^2)^2]\}^{1/2}$.

anion): 2.29 (tdt-Me), (4′-Me), 6.34, 7.04 (2′-,3′-H), 9.75, 13.95 (4-,6-Me), 15.45 (5-H).

$(Et_4N)_3$[$Fe_4S_4(LS_3)$(tdt)]. To a solution of 50 mg (26 μmol) of $(Et_4N)_2[Fe_4S_4(LS_3)(OTf)]$[20] in 20 mL of acetonitrile was added 12 mg (29 μmol) of $(Et_4N)_2$(tdt). The reaction mixture was stirred for 90 min and filtered, and the solvent was removed from the filtrate. The residue was washed with acetonitrile (1 mL) and ether (20 mL), affording the product as 37 mg (79%) of black solid. The ^{1}H NMR spectrum of the cluster was identical to that of the Ph_4P^+ salt prepared by a related method.[19]

$(Et_4N)_2$[$(Ph_3P)CuFe_3S_4(LS_3)$]. To a solution of 80 mg (49 μmol) of $(Et_4N)_3[Fe_3S_4(LS_3)]$ in 50 mL of acetonitrile was added 43 mg (49 μmol) of $[CuCl(PPh_3)_3]$.[21] The reaction mixture was stirred for 90 min and filtered, and the solvent was removed from the filtrate. The remaining solid was washed with ether (3 × 15 mL) and dried to give the product as 79 mg (88%) of black solid. The ^{1}H NMR spectrum is identical with that reported for this compound prepared by a different method.[18]

$(Et_4N)_3$[$(EtS)CuFe_3S_4(LS_3)$]. To a solution of 50 mg (28 μmol) of $(Et_4N)_2[(Ph_3P)CuFe_3S_4(LS_3)]$ in 20 mL of acetonitrile was added 25 mg (131 μmol) of (Et_4N)(SEt). The reaction mixture was stirred for 12 h and filtered. Solvent was removed from the filtrate, and the residue was washed with cold acetonitrile (10 mL, −30 °C) and dried. The product was obtained as 37 mg (77%) of black solid. ESMS: m/z 1888.7 $\{M + 4Et_4N\}^+$.

In the sections that follow, clusters are designated as **1**−**11** according to Chart 1.

X-ray Structure Determinations. Structures of the five compounds in Table 1 were determined. For simplicity, these compounds are referred to by their cluster designation. Diffraction-quality crystals were obtained by layering several volume equivalents of ether on Me_2SO solutions at room temperature. Crystals were coated with paratone-N oil and mounted on a Bruker APEX CCD-based diffractometer. Data were collected at 193 K with ω scans of 0.3°/frame for 30 s (60 s for **11**) using Mo Kα radiation. The number of frames collected for a hemisphere of data varied between 1305 and 1697. No significant decay, examined by recollection of the first 50 frames at the end of the data collection, was detected for any compound. Cell parameters were retrieved using SMART software for **6**, **9**, and **11**, and the CELL NOW program was used for twinned crystals of **5** and **7.** Refinement of cell parameters and correction for Lorentz and polarization effects were performed with SAINT. Absorption corrections were applied using SADABS for **11**, TWINABS for **5** and **7**, and the MULABS routine in PLATON for **6** and **9**. Space groups were assigned unambiguously by analysis of symmetry and systematic absences determined by XPREP. Compounds **5** and **7** occurred as twin crystals, each of them containing two microdomains. The twin laws were −1 0 0, 0 −1 0, 0 0 1 and −1 0 0, 0 −1 0, 0 0 −1 for **5** and **7**, respectively. Both of them contained one major component, as indicated by the batch scale factors (BASF) of 0.35 (**5**) and 0.31 (**7**). Missing symmetry in all crystals was checked with PLATON; none was found. Structures were solved by direct methods and refined against all data by full-matrix least-squares techniques on F^2 using the SHELXL-97 package. All non-hydrogen atoms were refined anisotropically. Hydrogen atoms were placed at idealized positions on carbon atoms. Crystal parameters and agreement factors are reported in Table 1.[23]

Chart 1. Designation of Clusters and Abbreviations

$[Fe_3S_4(LS_3)]^{3-}$	**1**[20]
$[(Ph_3P)NiFe_3S_4(LS_3)]^{2-}$	**2**[18]
$[(Bu^tNC)NiFe_3S_4(LS_3)]^{2-}$	**3**[17]
$[(dmpe)NiFe_3S_4(LS_3)]^{2-}$	**4**[16,17]
$[(EtS)NiFe_3S_4(LS_3)]^{3-}$	**5**
$[(HS)NiFe_3S_4(LS_3)]^{3-}$	**6**
$[(tdt)NiFe_3S_4(LS_3)]^{3-}$	**7**
$[(Ph_3P)CuFe_3S_4(LS_3)]^{2-}$	**8**[18]
$[(EtS)CuFe_3S_4(LS_3)]^{3-}$	**9**
$[Fe_4S_4(LS_3)Cl]^{2-}$	**10**[22]
$[Fe_4S_4(LS_3)(tdt)]^{3-}$	**11**[19]

bdt = benzene-1,2-dithiolate(2-), cod = cycloocta-1,5-diene, CODH = carbon monoxide dehydrogenase, dmpe = 1,2-bis(dimethylmethylphosphino)ethane, LS_3 = 1,3,5-tris((4,6-dimethyl-3-mercapto-phenyl)thio)-2,4,6-tris(*p*-tolylthio)benzene(3-), tdt = toluene-3,4-dithiolate(2-), TfO = triflate(1-), Tp = hydrotris(pyrazolyl)borate(1-)

The unit cell of compound **7** contains 4 cluster anions, 12 cations, and 3 solvate molecules. The Ni−tdt moiety is disordered in one of the two crystallographically independent anions at two positions in a 3:2 ratio. To assist convergence in refinement, the bond distances and angles of Ni−tdt were restrained to the same value for the two different positions, carbon atoms were fixed in idealized positions (C−C = 1.39 Å, C−C−C = 120°), and the methyl carbon atoms were fixed in the plane of the ring. Structural information

(21) Reichle, W. *Inorg. Chim. Acta* **1971**, *5*, 325−332.

(22) Stack, T. D. P.; Holm, R. H. *J. Am. Chem. Soc.* **1988**, *110*, 2484−2494.

(23) See the paragraph at the end of this article for available Supporting Information.

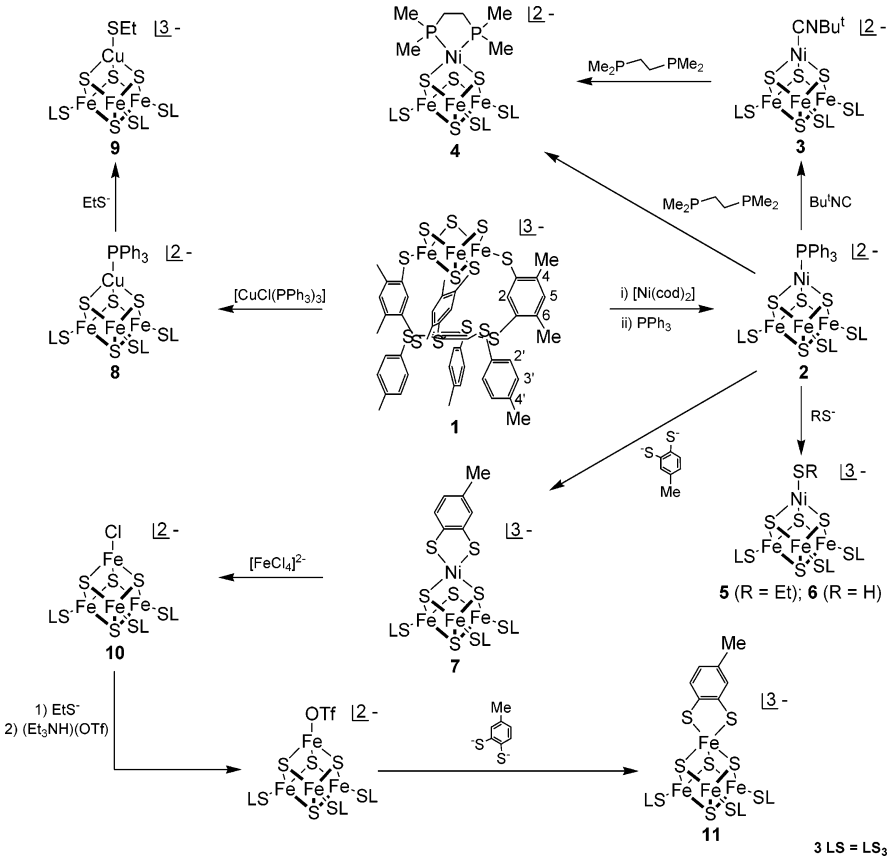

Figure 2. Scheme including present and previous results which summarizes the formation of clusters based on metalation of cuboidal cluster **1** and heterometal substitution reactions leading to nickel clusters **2**−**7** and copper clusters **8** and **9**. Also shown is the formation of iron cluster **11** from **10**. Note the ligand numbering scheme.

reported is confined to the non-disordered cluster. The SH ligand in **6** is disordered over two positions in a 3:2 occupancy ratio. In multiple crystallization experiments, cluster **9** was also isolated in the compound $(Et_4N)_3$[**9**]·1/2Me_2SO, whose structure was determined: orthorhombic, $P2_12_12_1$, $Z = 2$, $a = 14.9195(6)$ Å, $b = 18.4933(8)$ Å, $c = 33.457(2)$ Å, $V = 9231.1(7)$ Å^3, R1(wR2) = 8.06(17.33). Because the cluster structure was practically identical to that in the ·2Me_2SO crystal (Table 1), metric data are not reported.

Other Physical Measurements. All measurements were made under anaerobic conditions. Cyclic voltammograms were obtained with a Princeton Applied Research model 263 potentiostat/galvanostat using acetonitrile or Me_2SO solutions, a platinum working electrode, and 0.1 M $(Bu_4N)(ClO_4)$ supporting electrolyte. Potentials are referenced to a standard calomel electrode. Electrospray mass spectra were recorded on acetonitrile solutions directly infused into a LCT mass spectrometer at a flow rate of 5 μL/min.

Results and Discussion

While site-specific reactions of Fe_4S_4 clusters have been extensively documented in the course of developing a large manifold of 3:1 site-differentiated $[Fe_4S_4(LS_3)L']^{z-}$ clusters,[24−27] reactions at heterometal M sites in cubane-type MFe_3S_4 clusters have not been similarly examined. The first such reactions were those of $[(Ph_3P)NiFe_3S_4(SEt)_3]^{2-}$, where substitution of the phosphine was observed by ^{1}H NMR but no products were isolated.[28] In undertaking step (i) of the proposed C-cluster analogue synthesis, site-specific reactions at nickel and isolation of reaction products are required. In this work, we augment reaction 1 with several other reactions leading to thiolate ligation at the heterometal site and isolation of clusters. Product identification and characterization are provided by crystallographic structure proofs, ^{1}H NMR spectra, and other data pertinent to oxidation levels and redox properties.

Nickel(II) Site Reactions. Set out in Figure 2 are selected Ni^{II}-based substitution reactions from this and earlier work. The scheme originates with the cuboidal Fe_3S_4 cluster **1**.[20] As in previous reactivity studies,[16−18] we utilize the semirigid cavitand-like ligand LS_3[22] which stabilizes **1** and subsequent clusters and provides distinctive isotropically shifted ^{1}H NMR signals. All clusters were isolated as black, highly dioxygen-sensitive, Et_4N^+ salts. Cluster **1** upon reaction with $[Ni(cod)_2]$ and Ph_3P yields the $NiFe_3S_4$ cluster **2** (79%). This procedure is now the method of choice for the synthesis of **2**. The structure of the related cluster $[(Me_3P)NiFe_3S_4(LS_3)]^{2-}$ [17] has established the cubane-type structure and a tetrahedral Ni^{II} site. The phosphine is replaceable with Bu^tNC to yield **3**[17] and with dmpe to afford **4**.[16] Ethanethiolate and hydrosulfide

(24) Rao, P. V.; Holm, R. H. *Chem. Rev.* **2004**, *104*, 527−559.
(25) Holm, R. H.; Ciurli, S.; Weigel, J. A. *Progr. Inorg. Chem.* **1990**, *38*, 1−74.
(26) Weigel, J. A.; Holm, R. H. *J. Am. Chem. Soc.* **1991**, *113*, 4184−4191.
(27) Zhou, C.; Holm, R. H. *Inorg. Chem.* **1997**, *36*, 4066−4077.
(28) Ciurli, S.; Ross, P. K.; Scott, M. J.; Yu, S.-B.; Holm, R. H. *J. Am. Chem. Soc.* **1992**, *114*, 5415−5423.

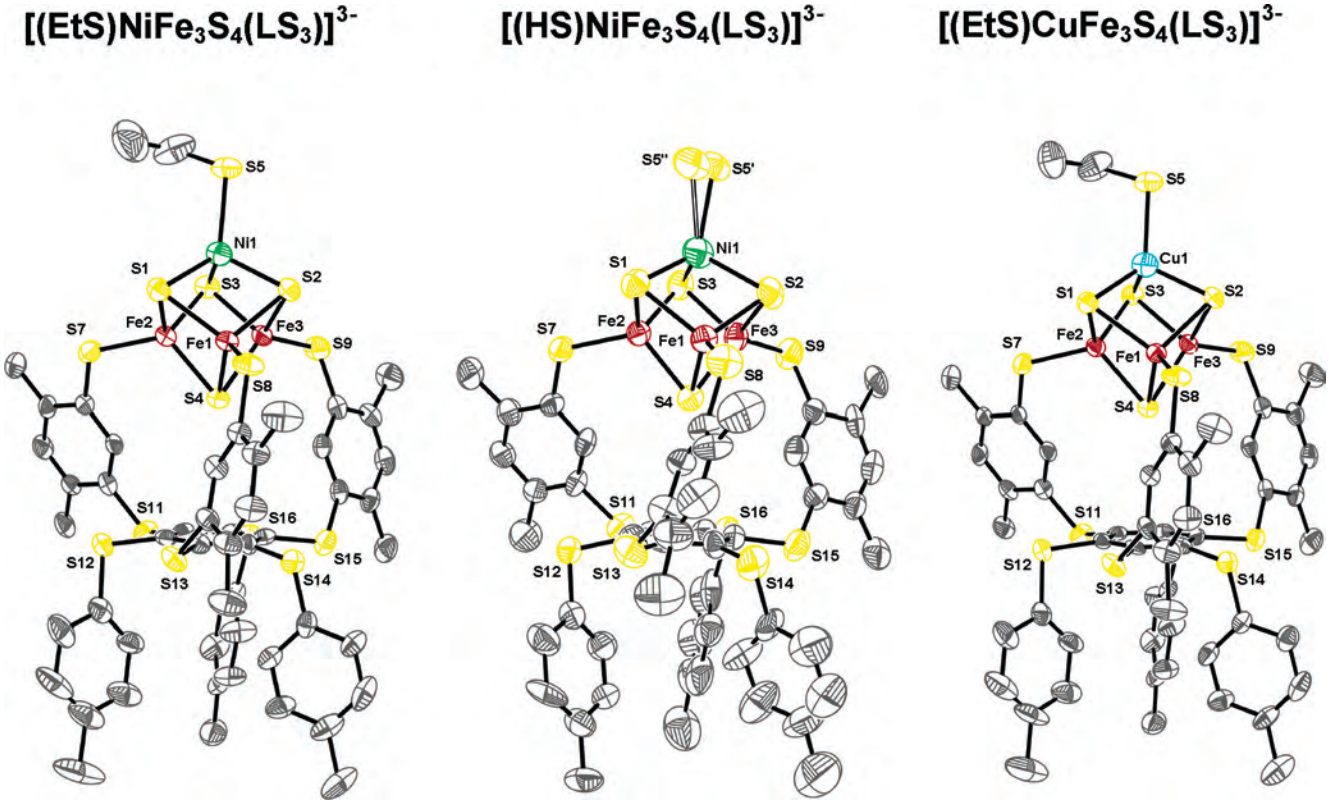

Figure 3. Structures of Ni^{II} and Cu^{I} clusters showing 50% probability ellipsoids and atom labeling schemes; selected (mean) values (Å) and ranges of values (deg) are given. $[(EtS)NiFe_3S_4(LS_3)]^{3-}$: Ni−SEt 2.296(2), Ni−($\mu_3$-S) 2.29(2), Fe−($\mu_3$-S) 2.29(1), Fe−$S_{terminal}$ 2.285(3), EtS−Ni-(μ_3-S) 110.1(1)−118.1(1), (μ_3-S)−Ni−(μ_3-S) 103.9(1)−105.3(1). $[(HS)NiFe_3S_4(LS_3)]^{3-}$: Ni−S5′ 2.284(7), Ni−($\mu_3$-S) 2.30(2), Fe−($\mu_3$-S) 2.30(1), Fe−$S_{terminal}$ 2.282(7), S5′−Ni−(μ_3-S) 106.8(2)−118.3(2), (μ_3-S)−Ni−(μ_3-S) 103.5(1)−106.3(1). $[(EtS)CuFe_3S_4(LS_3)]^{3-}$: Cu−SEt 2.280(2), Cu−($\mu_3$-S) 2.28(2), Fe−($\mu_3$-S) 2.33(3), Fe−$S_{terminal}$ 2.28(1), EtS−Cu−(μ_3-S) 110.6(1)−117.6(1), (μ_3-S)−Cu−(μ_3-S) 102.7(1)−105.8(1). All clusters have the *ababab* ligand conformation. The hydrosulfide ligand is disordered over two positions.

are now found to displace Ph_3P to yield clusters **5** (85%) and **6** (76%), respectively. These non-redox reactions preserve the $[NiFe_3S_4]^{1+}$ ($S = 3/2$) core. A similar reaction with toluene-3,4-dithiolate would be expected to produce $[(tdt)NiFe_3S_4(LS_3)]^{4-}$. However, as seen in reaction 2, the cluster actually isolated is trinegative **7** (65%). Under the conditions of isolation and crystallization, the putative 4− cluster has been oxidized to **7**.

$$[(Ph_3P)NiFe_3S_4(LS_3)]^{2-} + tdt^{2-} \rightarrow [(tdt)NiFe_3S_4(LS_3)]^{3-} + Ph_3P + e^- \quad (2)$$

Structure Proofs. (a) Cubane-Type Clusters. The structures of clusters **5**, **6**, and **9** have been determined and are provided in Figure 3. All clusters have the *ababab* ligand conformation with three coordinating arms above (*a*) and three buttressing *p*-tolylthio legs below (*b*) the central benzene ring, and all iron sites have a distorted tetrahedral configuration. Clusters **5** and **6**, as well as **7** (see below), are the first examples of isolated $NiFe_3S_4$ cubanes with thiolate or hydrosulfide ligation at the nickel site. The core structures are essentially identical with each other and with that of $[(Me_3P)NiFe_3S_4(LS_3)]^{2-}$.[17] Metric parameters are unexceptional, and (mean) values and ranges of metric parameters are summarized in Figure 3. The stereochemistry at the Ni^{II} sites is trigonally distorted tetrahedral. For **5**, ranges of EtS−Ni−S and intracore S−Ni−S angles are 110.0−118.1° and 103.9−105.3°, respectively, and Ni−SEt = 2.296(2) Å. For **6**, the corresponding ranges are 106.8−118.2° and 103.5−106.3°. The hydrosulfide ligand of **6** was found in two disordered positions which were modeled in a 3(S5′):2(S5′′) ratio. The Ni−S5′ distance of 2.284(7) Å closely conforms to the Ni−SEt bond length in **5**. Cluster **9**, with a similarly distorted tetrahedral Cu^{I} site, is essentially isostructural with **5**.

These results expand the structural database of cubane-type $NiFe_3S_4$ clusters to some five isoelectronic examples with effectively congruent core structures and variable terminal ligands at Ni^{II} (Ph_3P, Me_3P, EtS^-, HS^-).[17,29] Terminal hydrosulfide ligation, while not frequently encountered, has been established in other weak field cubane-type clusters including $[Fe_4S_4(LS_3)(SH)]^{2-}$,[30] $[Fe_4S_4(SH)_4]^{2-,3-}$,[31−33] and $[(Tp)MoFe_3S_4(SH)_3]^{2-}$,[34] and in $[(Tp)_2M_2Fe_6S_9(SH)_2]^{3-,4-}$ (M = Mo, V).[34,35] Cluster **9** is the first structurally characterized example of a cubane-type $CuFe_3S_4$ species.

(b) Cubanoid Cluster and Cubane-Type Cluster with a Five-Coordinate Site. The pertinent clusters are **7** and

(29) Zhou, J.; Scott, M. J.; Hu, Z.; Peng, G.; Münck, E.; Holm, R. H. *J. Am. Chem. Soc.* **1992**, *114*, 10843−10854.
(30) Cai, L.; Holm, R. H. *J. Am. Chem. Soc.* **1994**, *116*, 7177−7188.
(31) Hoveyda, H. R.; Holm, R. H. *Inorg. Chem.* **1997**, *36*, 4571−4578.
(32) Segal, B. M.; Hoveyda, H. R.; Holm, R. H. *Inorg. Chem.* **1998**, *37*, 3440−3443.
(33) Müller, A.; Schladerbeck, N.; Bögge, H. *J. Chem. Soc. Chem. Commun.* **1987**, 35−36.
(34) Zhang, Y.; Holm, R. H. *J. Am. Chem. Soc.* **2003**, *125*, 3910−3920.
(35) Zuo, J.-L.; Zhou, H.-C.; Holm, R. H. *Inorg. Chem.* **2003**, 4624−4631.

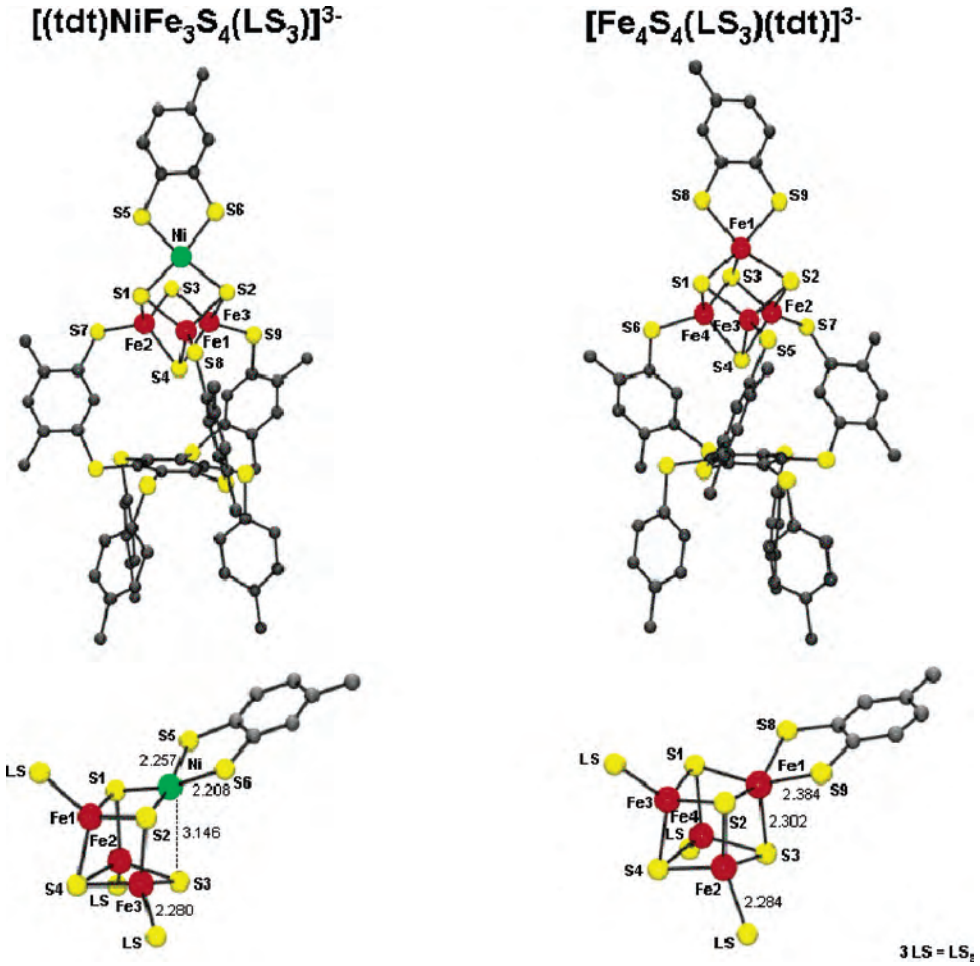

Figure 4. Structures of $[(tdt)NiFe_3S_4(LS_3)]^{3-}$ and $[Fe_4S_4(LS_3)(tdt)]^{3-}$. Upper: complete structures showing the *ababab* ligand conformations and atom labeling scheme. Lower: cluster portions showing selected (mean) bond lengths (Å) and emphasizing the large difference in the axial separations Ni···S3 and Fe1−S3.

11, both of which contain a M(tdt) fragment (M = Ni, Fe). Structures are shown in Figure 4, and metric parameters are collected in Table 2.

The most significant difference between the structures of **5**/**6** and **7** is the presence of an approximately planar Ni^{II} site in the latter. The long Ni···S3 distance of 3.146(7) Å emphasizes four-coordination which, however, is not strictly planar. Sulfur atom deviations from the NiS1S2S5S6 mean plane average to ±0.087(6) Å while the nickel atom is displaced 0.238(4) Å toward S3. The dihedral angle between coordination planes NiS1S2/NiS5S6 is 161.2(2)°. The top face of the cluster is nearly coplanar, the dihedral angle NiS1S2/Fe1S1S2 being 175.0(2)°. Portions of the top and bottom cluster faces are bent away from each other, forming an NiS1S2/Fe2Fe3S3 dihedral angle of 148.2(2)°. The tdt ligand is unsymmetrically chelated, with Ni−S distances of 2.208(5) and 2.257(5) Å. These values are somewhat larger than those of planar diamagnetic $Ni^{II}S_4$ complexes, including $[Ni(bdt)_2]^{2-}$ derivatives (2.17 Å)[36,37] and $[Ni(tdt)_2]^{2-}$ (2.19 Å),[38] and are comparable to that for a planar arylthiolate

Table 2. Selected Structural Parameters of $[Fe_4S_4(LS_3)(tdt)]^{3-}$ and $[(tdt)NiFe_3S_4(LS_3)]^{3-}$

	$[Fe_4S_4(LS_3)(tdt)]^{3-}$		
Fe1−S8	2.382(3)	Fe3−S4	2.235(2)
Fe1−S9	2.386(3)	Fe4−S1	2.225(3)
Fe1−S1	2.443(3)	Fe4−S3	2.297(3)
Fe1−S2	2.427(2)	Fe4−S4	2.309(2)
Fe1−S3	2.302(3)	mean of 9	2.28(3)
Fe2−S2	2.245(3)	Fe2−S7	2.281(3)
Fe2−S3	2.304(2)	Fe3−S5	2.282(3)
Fe2−S4	2.304(2)	Fe4−S6	2.290(3)
Fe3−S1	2.288(3)	mean of 3	2.284(5)
Fe3−S2	2.289(2)		
S8−Fe1−S9	84.21(9)	S3−Fe1−S8	112.71(9)
S1−Fe1−S2	93.85(8)	S3−Fe1−S9	104.3(1)
S1−Fe1−S3	98.72(9)	S2−Fe1−S8	147.5(1)
S2−Fe1−S3	99.70(9)	S1−Fe1−S9	156.8(1)
Fe1S1S2/FeS8S9	140.6(1)	Fe1S1S2/Fe3S1S2	158.5(1)
	$[(tdt)NiFe_3S_4(LS_3)]^{3-}$		
Ni−S5	2.257(5)	Fe2−S4	2.283(4)
Ni−S6	2.208(5)	Fe3−S2	2.298(5)
Ni−S1	2.260(5)	Fe3−S3	2.229(5)
Ni−S2	2.286(5)	Fe3−S4	2.307(4)
Ni−S3	3.146(7)	mean of 9	2.27(3)
Fe1−S1	2.250(4)	Fe2−S7	2.263(5)
Fe1−S2	2.284(5)	Fe1−S8	2.295(4)
Fe1−S4	2.266(4)	Fe3−S9	2.285(5)
Fe2−S1	2.276(4)	mean of 3	2.28(2)
Fe2−S3	2.233(5)		
NiS1S2/NiS5S6	161.2(2)	NiS1S2/Fe2S3Fe3	148.2(2)
NiS1S2/Fe1S1S2	175.0(2)		

(36) Sellman, D.; Binder, H.; Häussinger, D.; Heinemann, F. W.; Sutter, J. *Inorg. Chim. Acta* **2000**, *300*−*302*., 829−836.
(37) Simão, D.; Alves, H.; Belo, D.; Rabaça, S.; Lopes, E. B.; Santos, I. C.; Gama, V.; Duarte, M. T.; Henriques, R. T.; Novais, H.; Almeida, M. *Eur. J. Inorg. Chem.* **2001**, 3119−3126.

Table 3. Redox Potentials of Fe_3S_4 and $NiFe_3S_4$ Clusters

cluster	$E_{1/2}$ (V)[a]			ref
	$[Fe_3S_4]^{1/0}$	$[Fe_3S_4]^{0/1+}$		
$[Fe_3S_4(LS_3)]^{3-}$ [b]	−1.67	−0.79		20
	$[Fe_4S_4]^{1+/2+}$	$[Fe_4S_4]^{2+/3+}$		
$[(tdt)Fe_4S_4(LS_3)]^{3-}$ [e]	−1.38	−0.66		19
	$[NiFe_3S_4]^{0/1+}$	$[NiFe_3S_4]^{1+/2+}$	$[NiFe_3S_4]^{2+/3+}$	
$[(Ph_3P)NiFe_3S_4(LS_3)]^{2-}$ [b]	−1.45	−0.42[c]	−	18
$[(EtS)NiFe_3S_4(LS_3)]^{3-}$ [b]	−1.81[d]	−0.73	−	*f*
$[(dmpe)NiFe_3S_4(LS_3)]^{2-}$	−	−1.03	−0.01[c]	16
$[(tdt)NiFe_3S_4(LS_3)]^{3-}$	−	−1.30	−0.75[c]	*f*
	$[CuFe_3S_4]^{0/1+}$	$[CuFe_3S_4]^{1+/2+}$		
$[(Ph_3P)CuFe_3S_4(LS_3)]^{2-}$ [b]	−1.35	−0.38[c]		18
$[(NC)CuFe_3S_4(LS_3)]^{3-}$ [b]	−1.50	−0.52		18
$[(EtS)CuFe_3S_4(LS_3)]^{3-}$ [e]	−1.60	−0.66		*f*

[a] Versus SCE at 298 K. [b] Acetonitrile. [c] E_{pa}, irreversible. [d] E_{pc}, irreversible. [e] Me_2SO. [f] This work

Table 4. Mössbauer Parameters and ^1H Isotropic Shifts of Fe_3S_4 and MFe_3S_4 Clusters (M = Ni, Cu)

				$(\Delta H/H_0)_{iso}$[c]			
cluster	*S*	δ(mm/s)[a]	ΔE_Q (mm/s)[b]	4-Me	5-H	6-Me	ref
$[Fe_3S_4(LS_3)]^{3-}$	2	0.35, 0.48, 0.49	1.48, 1.18, 0.51	−6.69	−8.69	−9.61[d]	20
$[(Ph_3P)NiFe_3S_4(LS_3)]^{2-}$	3/2	0.56	1.23	−6.47	−7.74	−9.79[d]	*g*, 16
$[(EtS)NiFe_3S_4(LS_3)]^{3-}$	3/2	0.56(1), 0.52(2.5)	2.21(1), 1.17(2)	−5.73	−7.54	−8.55[d]	*g*
$[(dmpe)NiFe_3S_4(LS_3)]^{2-}$	5/2	0.64(1), 0.54(2)[f]	2.74(1), 1.36(2)	−11.29	−11.56	−15.12[e]	16, 17
$[(tdt)NiFe_3S_4(LS_3)]^{3-}$	2	0.49	1.18	−7.89	−8.56	−11.80[d]	*g*
$[(tdt)Fe_4S_4(LS_3)]^{3-}$	0	0.52(1), 0.37(1.6) 0.36(1.4)	1.97(1), 0.96(1.6) 1.29(1.4)	−1.65	−1.54	−2.03[d]	19
$[(Ph_3P)CuFe_3S_4(LS_3)]^{2-}$	2	*h*		−7.90	−9.52	−11.68[e]	18
$[(NC)CuFe_3S_4(LS_3)]^{3-}$	2	*h*		−7.25	−9.18	−11.08[e]	*g*
$[(EtS)CuFe_3S_4(LS_3)]^{3-}$	2	0.33(1), 0.48 (1.6)	1.29(1), 0.68(1.6)	[h]			*g*

[a] 4.2 K, ±0.02 mm/s; isomer shifts vs Fe metal at room temperature. [b] ±0.03 mm/s. [c] Room temperature; $(\Delta H/H_0)_{iso} = (\Delta H/H_0)_{dia} - (\Delta/H_0)_{obs}$; diamagnetic references are $(Bu_4N)(LS_3)$ in MeCN and $Na_3(LS_3)$ in Me_2SO. [d] Me_2SO. [e] MeCN. [f] 77 K. [g] This work. [h] Not determined.

complex (2.22 Å),[39] but are less than nearly all Ni−S bond lengths in three structures of paramagnetic distorted tetrahedral $[Ni(SPh)_4]^{2-}$ (2.26−2.33 Å).[40−42] The Ni-(μ_3-S) distances of 2.260(5) and 2.286(5) Å do overlap with the lower end of the tetrahedral range in **5**, **6**, and several other mononuclear complexes. The emerging picture is that of a diamagnetic coordination unit with a nonplanar distortion and a presumably weaker ligand field than in conventional planar $Ni^{II}S_4$ complexes, for which the normal bond distance range is 2.16−2.22 Å.

In order to provide a structural comparison with **7**, iron cluster **11** was prepared from **10** by the procedure in Figure 2 and isolated as the Et_4N^+ salt (79%). The cluster had been previously prepared as the Ph_4P^+ salt from **10** and Li_2(bdt) in acetonitrile.[19] Its structure reveals retention of the cubane-type core with the same mean Fe-(μ_3-S) and terminal Fe−S distances as in **7** (Figure 4, Table 2). The tdt ligand is symmetrically bound to Fe1, which exhibits approximate square pyramidal coordination similar to that in dinuclear Fe^{III} complexes such as $[Fe_2(bdt)_4]^{2-}$ and $[Fe_2(tdt)_4]^{2-}$.[43−45] In this description, atoms S1S2S8S9 define the basal plane and S3 is in the axial position. Atom Fe4 is displaced from this plane toward S3 by 0.569(2) Å. The axial Fe1−S3 bond distance is 2.302(3) Å, 0.84 Å shorter than the Ni···S axial separation.

Clusters **7** and **11** display contrasting geometries of MFe_3S_4 clusters when the heterometal sites are planar and five-coordinate, respectively. The structure of **7** clearly approaches that of the *Ch* CODH II C-cluster (Figure 1) with tdt coordination simulating S_{Cys} and μ_2-S binding at the nickel site.

Oxidation States and Redox Properties. These properties are examined with reference to the redox potentials, ^{57}Fe isomer shifts, and ^1H NMR isotropic shifts contained in Tables 3 and 4. Isomer shifts given below are weighted mean values. Cuboidal cluster **1**, the precursor to all other clusters in Figure 2, displays reversible oxidation and reduction steps. Introduction of a Cu^IL group into the $[Fe_3S_4]^0$ core affords the $[CuFe_3S_4]^{1+}$ core. Isomer shifts of **1** (0.44 mm/s) and **9** (0.42 mm/s) indicate the same iron oxidation state ($Fe^{2.67+}$), as would be expected from inclusion of Cu^I. Potentials of **1** and **9** are nearly the same at parity of cluster charge (3−) and are less negative in $[(Ph_3P)CuFe_3S_4(LS_3)]^{2-}$.

The situation is different with clusters **2** and **5** and by implication for **3** and **6**. The formulation $[NiFe_3S_4]^{1+}$ ($S = 3/2$) ≡ Ni^{2+} ($S = 1$) + $[Fe_3S_4]^{1-}$ ($S = 5/2$), where the cluster system spin arises from antiferromagnetic coupling of component spins, has been demonstrated with closely related clus-

(38) Lindahl, P. A.; Kojima, N.; Hausinger, R. P.; Fox, J. A.; Teo, B. K.; Walsh, C. T.; Orme-Johnson, W. H. *J. Am. Chem. Soc.* **1984**, *106*, 3062−3064.
(39) Erkizia, E.; Conry, R. R. *Inorg. Chem.* **2000**, *39*, 1674−1679.
(40) Swenson, D.; Baenziger, N. C.; Coucouvanis, D. *J. Am. Chem. Soc.* **1978**, *100*, 1932−1934.
(41) Yamamura, T.; Miyamae, H.; Katayama, Y.; Sasaki, Y. *Chem. Lett.* **1985**, 269−272.
(42) Rheingold, A. L.; Beall, K. S.; Riggs, P. J.; Groh, S. E. *Acta Crystallogr.* **1993**, *C49*, 542−543.
(43) Sawyer, D. T.; Srivasta, G. S.; Bodini, M. E.; Schaefer, W. P.; Wing, R. M. *J. Am. Chem. Soc.* **1986**, *108*, 936−942.
(44) Wong, L.; Kang, B. *Jiegou Huaxue (J. Struct. Chem.)* **1987**, *6*, 94−97.
(45) Sellman, D.; Peters, K. P.; Molina, R. M.; Heinemann, F. W. *Eur. J. Inorg. Chem.* **2003**, 903−907.

ters.[29,46,47] The isomer shifts of 0.56 (**2**) and 0.53 mm/s (**5**) are indistinguishable from 0.55 mm/s for protein-bound $[ZnFe_3S_4]^{1+}$ ($S = 5/2$)[47] with a likely cubane-type geometry. The isomer shift and spin state of cluster **4** (0.57 mm/s) are also indicative of the $[NiFe_3S_4]^{1+}$ state but with planar diamagnetic Ni^{2+}. Clusters **2** and **5** each exhibit a reduction step at rather negative potential to generate all-ferrous $[NiFe_3S_4]^0$ species, which have never been isolated, and an oxidation step to form the $[NiFe_3S_4]^{2+}$ state. The isomer shift 0.49 mm/s for cluster **7** and the composition of the Et_4N^+ salt found in the X-ray structure are indicative of the formulation $[NiFe_3S_4]^{2+} \equiv Ni^{2+}$ ($S = 0$) + $[Fe_3S_4]^0$ ($S = 2$). This cluster ($Fe^{2.67+}$) is more oxidized than **4** ($Fe^{2.33+}$). The low potential of −1.30 V for the $[(tdt)NiFe_3S_4(LS_3)]^{4-/3-}$ couple (Table 3) facilitates oxidation of the presumed initial 4− reaction product over the course of isolation and crystallization, affording as the product $(Et_4N)_3$ [**7**]. We have recently encountered similar oxidations of other low-potential 4− clusters upon isolation and crystallization despite anaerobic conditions.[48]

Isotropic shifts of all Fe_4S_4 and MFe_3S_4 clusters examined to date are dominantly or fully contact in origin, i.e., $(\Delta H/H_0)_{iso} \cong (\Delta H/H_0)_{con}$ and therefore are proportional to magnetic susceptibility.[49] For a molecule of spin S, $(\Delta H/H_0)_{con} = -(A_i/\hbar)[g_{av}^2\mu_B^2 S(S+1)/3\gamma_N kT]$, where the symbols have their usual meaning. For $[Fe_4S_4]^{2+}$ clusters such as **11**, which have a diamagnetic ground state, the expression must be modified to include thermal occupation of excited paramagnetic states.[49−51] The contact nature of the shifts is readily seen from the results for iron cluster **11**; note the ligand numbering scheme in Figure 2. Briefly, ligand-to-metal antiparallel spin transfer creates positive spin density at C2, C4, and C6 and negative spin density at C5 of the odd-alternate phenylthiolate arm. From the McConnell equation $A_i = Q\rho_C^{\pi}$ with A_{CH} negative and A_{CCH3} positive, 4-Me, 5-H, and 6-Me should exhibit negative shifts, as observed (Table 4). The predicted signs of isotropic shifts has been demonstrated for the clusters $[Fe_4S_4(SC_6H_4Me)_4]^{2-,3-}$ with *o*-, *m*-, and *p*-Me substituents.[50] All other clusters in Table 4 also exhibit negative isotropic shifts, indicating that they are mainly contact shifts. Figure 5 contains illustrative spectra of **2**, **4**, and **7** in the downfield region. Our experience with $[Fe_4S_4(LS_3)L'_n]^{z-}$and $[L'_nMFe_3S_4(LS_3)]^{z-}$ clusters is that 4-Me and 6-Me chemical shifts are more sensitive to solvent and ligand(s) L′, possibly because of the more exposed positions of methyl groups, than are 5-H shifts. In the case of cluster **7**, isotropic shifts of the three substituents vary linearly with $1/T$ at 298−353 K in Me_2SO solution and the 5-H shift extrapolates accurately to a near-zero value at $1/T \cong 0$. Consequently, we take 5-H shifts as best reflecting contact interactions and magnetic susceptibilities. We find that 5-H isotropic shifts increase in the order $S = 0$ (**11**) < $S = 3/2$ (**2**, **5**) < $S = 2$ (**1**, **7**, **8**, $[(NC)CuFe_3S_4(LS_3)]^{3-}$ < $S = 5/2$ (**4**). Note also that all shifts of **4** are larger than for any other cluster. These results provide additional evidence that cluster **7** contains the above $[NiFe_3S_4]^{2+}$ core oxidation level and is more oxidized than cluster **4**.[52]

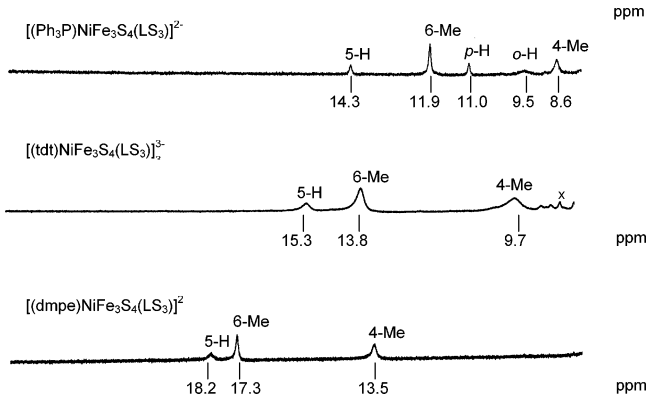

Figure 5. ^{1}H NMR spectra at 298 K of $[(Ph_3P)NiFe_3S_4(LS_3)]^{2-}$ ($S = 3/2$) and $[(tdt)NiFe_3S_4(LS_3)]^{3-}$ ($S = 2$) in Me_2SO-d_6 and of $[(dmpe)NiFe_3S_4(LS_3)]^{2-}$ ($S = 5/2$) in acetonitrile showing the effect of spin state on 4-Me, 5-H, and 6-Me shifts.

Summary. The following are the principal results and conclusions of this investigation, including certain results from earlier studies.[16,17]

(1) The cubane-type cluster $[(Ph_3P)NiFe_3S_4(LS_3)]^{2-}$ supports substitution reactions with phosphine displacement by thiolate ligands to yield clusters with tetrahedral ($[(RS)NiFe_3S_4(LS_3)]^{3-}$) or planar ($[(tdt)NiFe_3S_4(LS_3)]^{3-}$) stereochemistry at the nickel site, demonstrating that thiolate ligands can be bound at that site. Clusters with oxidation levels $[NiFe_3S_4]^{1+}$ ($S = 3/2$, 5/2) and $[NiFe_3S_4]^{2+}$ ($S = 2$) have been isolated.

(2) The chelate ligands dmpe and tdt form the clusters $[(dmpe)NiFe_3S_4(LS_3)]^{2-}$ and $[(tdt)NiFe_3S_4(LS_3)]^{3-}$, respectively, accommodating the $NiFe_3(\mu_2\text{-}S)(\mu_3\text{-}S)_3$ cubanoid core and approximately planar Ni^{II} sites. This core structure is common to all crystallographic C-cluster models.[13] The Ni(tdt)$(\mu_3\text{-}S)_2$ coordination unit with a Ni···S separation of 3.15 Å from an axial sulfur atom is a rendition of the Ni$(\mu_2\text{-}S)(\mu_3\text{-}S)_2(S_{Cys})$ unit of *Ch* CODH II.

(3) On the basis of structural and Mössbauer and ^{1}H NMR spectroscopic results, the core of $[(tdt)NiFe_3S_4(LS_3)]^{3-}$ is formulated as $[NiFe_3S_4]^{2-} \equiv Ni^{2+}$ ($S = 0$) + $[Fe_3S_4]^0$ ($S = 2$). This cluster is one electron more oxidized than $[(dmpe)NiFe_3S_4(LS_3)]^{2-}$, whose core is formulated as $[NiFe_3S_4]^{1+}$ ($S = 3/2$) $\equiv Ni^{2+}$ ($S = 1$) + $[Fe_3S_4]^{1-}$ ($S = 5/2$). The low redox potential of this cluster facilitates oxidation of the 4− cluster, which was not isolated.

(4) $[(tdt)NiFe_3S_4(LS_3)]^{3-}$ is the closest synthetic approach to a C-cluster but lacks the exo iron atom.

The results in (2) demonstrate the feasibility of a planar NiS_4 site in a cubanoid $NiFe_3S_4$ cluster and raise the

(46) Johnson, M. K.; Duderstadt, R. E.; Duin, E. C. *Adv. Inorg. Chem.* **1999**, *47*, 1−82.
(47) Srivastava, K. K. P.; Surerus, K. K.; Conover, R. C.; Johnson, M. K.; Park, J.-B.; Adams, M. W. W.; Münck, E. *Inorg. Chem.* **1993**, *32*, 927−936.
(48) Berlinguette, C. P.; Miyaji, T.; Zhang, Y.; Holm, R. H. *Inorg. Chem.* **2006**, *45*, 1997−2007.
(49) Bertini, I.; Luchinat, C. *NMR of Paramagnetic Molecules in Biological Systems*; Benjamin/Cummings Publishing Co., Inc.: Menlo Park, CA, 1986; Chapter 2.
(50) Reynolds, J. G.; Laskowski, E. J.; Holm, R. H. *J. Am. Chem. Soc.* **1978**, *100*, 5315−5322.
(51) Bertini, I.; Turano, P.; Vila, A. J. *Chem. Rev.* **1993**, *93*, 2833−2932.

(52) While the order of shifts with total spin S clearly indicates a relation to magnetic susceptibility, the shifts cannot be scaled according to the above equation because values of g_{av} and A_i are not known.

possibility of incorporation of an exo iron atom through sulfur bridging in $[(tdt)NiFe_3S_4(LS_3)]^{3-}$ or other clusters prepared by the substitution reactions such as those of (1). This issue is currently under investigation.

Acknowledgment. This research was supported by NIH Grant No. GM 28856. C.T. was supported by a fellowship from the Quebec Nature and Technology Research Fund. We thank Dr. R. Panda for preliminary observations and helpful discussions.

Supporting Information Available: X-ray crystallographic files in CIF format for the five compounds in Table 1. This material is available free of charge via the Internet at http://pubs.acs.org.

IC062362Z